CHIN. PHYS. LETT. Vol. 26, No. 11 (2009) 118501

Bilayer Photoresist Insulator for High Performance Organic Thin-Film Transistors on Plastic Films *

WANG He(王贺)[1,2], LI Chun-Hong(李春红)[1], PAN Feng(潘峰)[1], WANG Hai-Bo(王海波)[1], YAN Dong-Hang(闫东航)[1]**

[1]*State Key Laboratory of Polymer Physics and Chemistry, Changchun Institute of Applied Chemistry, Chinese Academy of Sciences, Changchun 130022*

[2]*Graduate School of Chinese Academy of Sciences, Beijing 100049*

(Received 26 June 2009)

A novel bilayer photoresist insulator is applied in flexible vanadyl-phthalocyanine (VOPc) organic thin-film transistors (OTFTs). The micron-size patterns of this photoresisit insulator can be directly defined only by photolithography without the etching process. Furthermore, these OTFTs exhibit high field-effect mobility (about 0.8 cm^2/Vs) and current on/off ratio (about 10^6). In particular, they show rather low hysteresis (< 1 V). The results demonstrate that this bilayer photoresist insulator can be applied in large-area electronics and in the facilitation of patterning insulators.

PACS: 85. 30. Tv, 72. 80. Le, 72. 80. Sk

In the research of organic thin-film transistors (OTFTs) in the last two decades, the gate insulator has been widely studied due to their important effect on the performance of the OTFTs.[1,2] Especially, the bilayer insulators have been effectively utilized to improve the performance of the OTFTs.[3,4] Therein, the polymer bilayer insulators implemented by solution fabrication[5−10] can avoid the problems with the single-layer organic insulator, such as leakage current and hysteresis.[11,12] The polymer bilayer insulators usually consist of a thin dielectric which helps to induce good electrical characteristics and a thicker dielectric with good dielectric properties. In practical applications, the present insulators are generally patterned by two traditional processes, i.e. photolithography and etching. Photolithography is the process of transferring patterns of geometric shapes on a mask to a thin layer of radiation-sensitive material (photoresist) covering the surface of insulator. The photoresist patterns defining the various regions are not permanent elements of the final device but only replicas of insulator features. To produce insulator features, these photoresist patterns must be transferred once more into the underlying insulators. The pattern transfer is accomplished by an etching process that selectively removes unmasked portions of the insulators.[13] For some radiation-sensitive polymers, it is possible that the pattern procedure of the insulator can be accomplished by photolithography. Therefore, a radiation-sensitive bilayer insulator will contribute to cost saving and have promising future in organic electronics.

In this Letter, we report a bilayer photoresist insulator comprising two radiation-sensitive materials, i.e. polyvinylalchohol (PVA) and benzocyclobutenone derivative (BCBO(III)).[14] This insulator patterns can be directly defined only by the photolithography without etching process, even at micro-size level. The VOPc OTFTs with the bilayer photoresist insulator have also been fabricated on the plastic films and exhibited excellent performances. The field-effect mobility reaches 0.78 cm^2/Vs, leakage current is about 10^{-10} A and the negligible hysteresis voltage is less than 1 V.

The pattern procedure of the bilayer photoresisit insulator is shown in Fig. 1(a). The PVA (molecule weight M_w is 46000–186000) was purchased from Aldrich Company. The BCBO(III) (molecule weight M_w is 5000–30000) sample was synthesized in the laboratory[14] and the molecular structure was given in Fig. 1(b). Firstly, 4% aqueous PVA solution including 1% ammonium dichromate photosensitizer was spin-coated on the polyethylene teraphythalate (PET) films with aluminum (Al) gate. The PVA film was patterned according to the reported procedure[15] and has a thickness of 660 nm. Secondly, 1% BCBO(III) tetrahydrofuran (THF) solution was spin-coated and baked at 70°C for 5 min. The BCBO(III) film was patterned by UV exposure through a mask, which was followed by developing in acetone. After being baked at 170°C for 10 min, 120 nm BCBO(III) film was formed. Thereafter, the VOPc active layers were formed on ordered para-sexiphenyl (p-6P) layer by weak epitaxy growth method.[16] The p-6P and VOPc were deposited at the substrate temperatures of 170°C and 150°C, respectively. In the end, the gold source and drain electrodes were thermally deposited through a shadow mask. The channel length L and width W were 100 μm and 3000 μm, respectively. To esti-

*Supported by the National Natural Science Foundation of China under Grant Nos 50773079, 50803063 and 20621401, and the National Basic Research Program of China under Grant No 2009CB939702.

**Email: yandh@ciac.jl.cn

© 2009 Chinese Physical Society and IOP Publishing Ltd

mate the dielectric constant κ, metal-insulator-metal (MIM) capacitors with 2-mm-diameter electrode were also fabricated. The electrical characterizations of OTFTs and MIM capacitors were measured in air by using two Keithley 236 source-measurement units and an Agilent E4980A LCR meter, respectively. The thickness and roughness of the film were measured by the tapping-mode atomic force microscopy (Quesant 250).

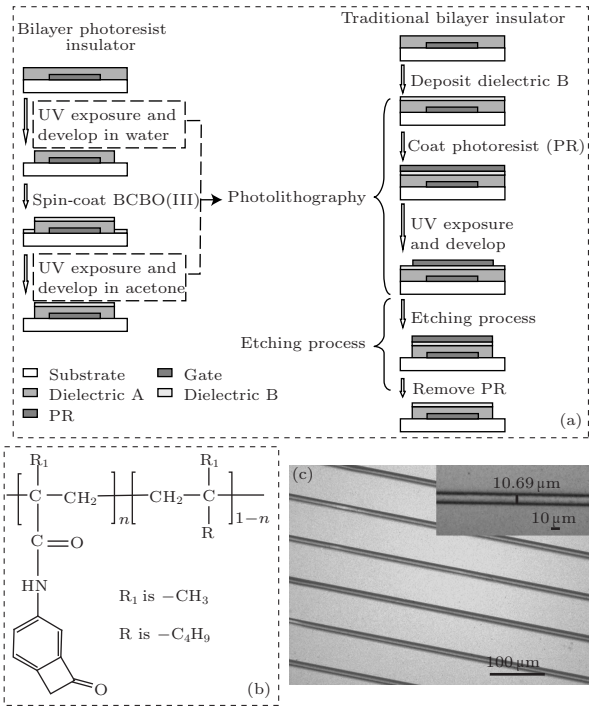


Fig. 1. (a) Schematic illustration of the patterning procedures of the traditional bilayer insulator and bilayer photoresist insulator. In the bilayer photoresist insulator, dielectric A is PVA and dielectric B is BCBO(Ⅲ). (b) The molecular structures of BCBO(Ⅲ). (c) The optical micrographs of 10 μm wide grooves of the bilayer phtotoresist insulator. Bright: bilayer insulator, Dark: Al.

The patterning procedures of the bilayer photoresist insulator and the traditional bilayer insulator are compared in Fig. 1(a). The patterning procedure of the former was implemented without the etching process, which was simpler than that of the latter. This is because the bilayer photoresist insulator comprises radiation-sensitive dielectrics and the patterns defined by the photolithographic process can be used as permanent elements of the final device. In Fig. 1(c), 10-μm-wide grooves made in the bilayer photoresist insulator are shown. This size-level pattern can meet the need of the displays. Moreover, microtopographs of the grooves were also measured by an atomic force microscope (AFM). The rms surface roughness of the insulator is about 0.5 nm, and of the groove (Al film) is about 1.1 nm which almost equals to that of the fresh Al film on the PET film. The results indicate that the bilayer insulator formed by the photoresists, i.e. PVA and BCBO(III), has smooth surface and is able to be removed clearly. Therefore, the patterns with the same precision can be obtained only by a one-step patterning procedure using this bilayer photoresist insulator rather than a two-step procedure using the traditional bilayer insulator.

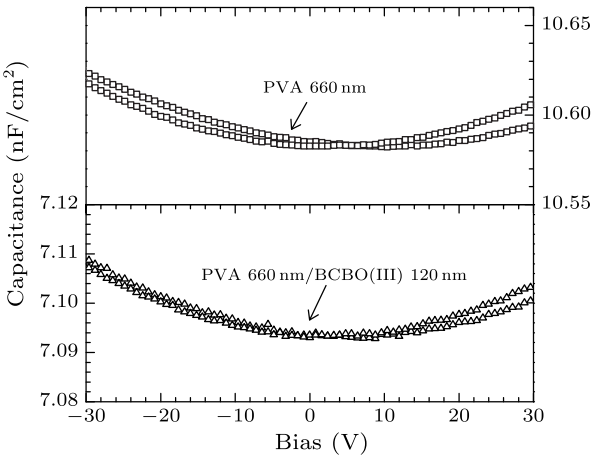


Fig. 2. Capacitance C vs voltage V for 660-nm-thick PVA single layer and 780-nm-thick bilayer photoresisit insulators on the PET films as measured from 2-mm-diameter Al dot/dielectric/Al structures at 1 kHz.

Figure 2 depicts the characteristics of capacitance C vs voltage V for the PVA (660 nm) single dielectric layer and the bilayer photoresist insulator at a frequency of 1 kHz, which were measured with the bias sweeping from +30 to −30 V and then back from −30 to +30 V. The capacitances of the PVA and the bilayer photoresist insulators are about 10.5 nF/cm^2 and 7 nF/cm^2, respectively. The dielectric constant κ of the PVA and the bilayer photoresist insulator are estimated from the measured capacitance values, which are 7.5 and 6, respectively. Under various bias sweeps, the capacitance difference is found in the PVA single layer but not in the bilayer photoresist insulator, which demonstrates that the latter has better bias stability.

The transfer characteristics of the p-6P / VOPc OTFTs with the PVA single layer and the bilayer photoresist insulators on PET films at a constant source-drain voltage of −30 V are shown in Figs. 3(a) and 3(b), respectively. The field-effect hole mobility μ and threshold voltage V_T are estimated in the saturations as follows:

$$I_{\rm DS} = \frac{W}{2L}\mu C_i(V_{\rm GS} - V_T)^2, \qquad (1)$$

where $I_{\rm DS}$ is the source-drain current density; W and L are the channel width and length, respectively; C_i is the insulator capacitance, and $V_{\rm GS}$ and V_T are the gate-source voltage and threshold voltage, respectively.[13] The field-effect characteristics of the OTFTs with the PVA single layer and the bilayer photoresist insulators are summarized in Table 1, which

are estimated when the gate voltage is swept from +10 to −30 V and then from −30 to +10 V at a constant source-drain voltage of −30 V. The hysteresis effect is scaled with the difference of the threshold voltage in various gate sweeps.[17] The OTFTs with the PVA single layer insulator show a high mobility of about 0.8 cm^2/Vs, while those with bilayer photoresist insulator show about 0.2 cm^2/Vs. However, the former has a larger hysteresis effect of 5.5 V while the latter less than 1 V which approaches to the level of the TFTs based on amorphous silicon. Moreover, the maximum gate leakage current (source-gate current) also reduced by three orders of magnitude (from 10^{-7} A to 10^{-10} A), as shown in Fig. 3(c). We optimize the performance of the OTFTs with the bilayer photoresist insulator by increasing the substrate temperature. At substrate temperature 170°C, the highest processing temperature of our PET substrate, the best-performance OTFTs have been obtained and their typical output characteristics are given in Fig. 3(d). With increasing V_{DS}, the linear region and saturation region are observed obviously. The OTFTs exhibit a field-effect mobility of about 0.78 cm^2/Vs, an on/off current ratio of about 10^6 and a threshold voltage of −10 V, which are estimated by Eq. (1) at a constant source-drain voltage of −30 V.

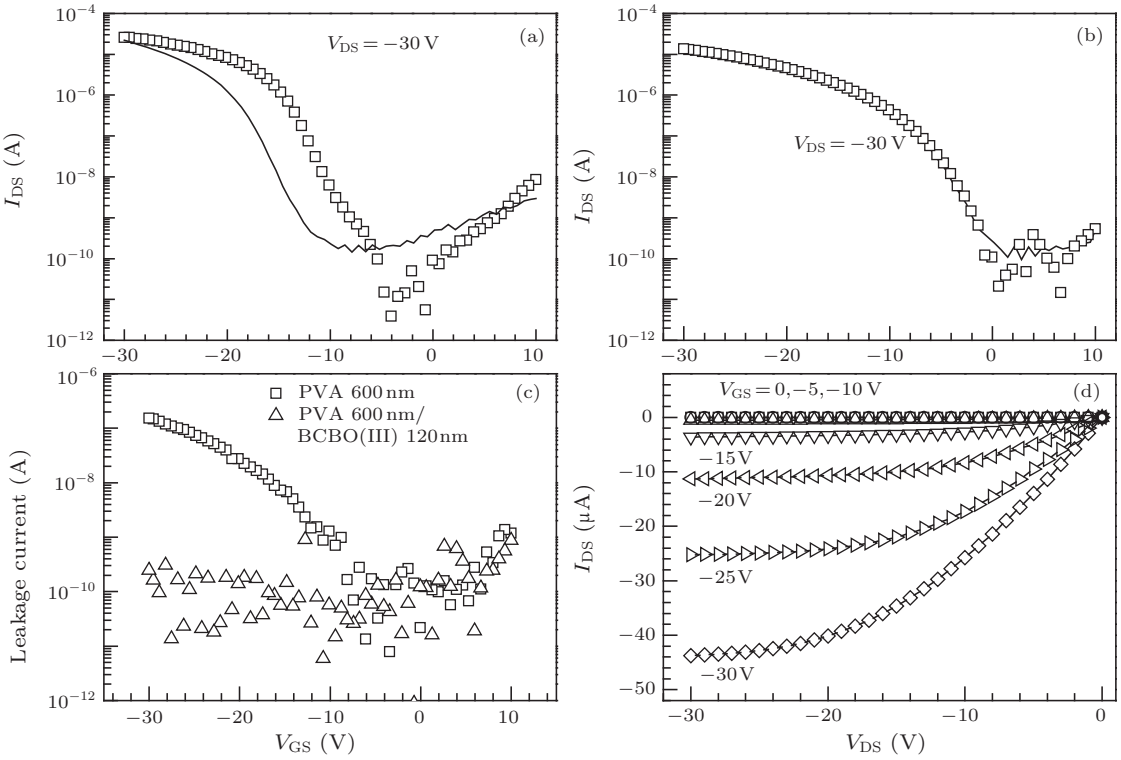


Fig. 3. Transfer characteristics of the OTFTs with (a) 660-nm-thick PVA single layer insulator and (b) 780-nm-thick bilayer photoresist insulator. The drain-source voltage is −30 V. The voltage sweep is from +10 to −30 V (symbol) and vice versa (line). (c) The leakage current of the OTFTs with single and double layer insulators. (d) The output characteristics at different gate voltages for optimized OTFTs with bilayer photoresist insulator.

Table 1. Field-effect characteristics of the OTFTs. Here minus denotes the gate voltage sweeping from +10 to −30 V and plus represents the gate voltage sweeping from −30 to +10 V.

Insulator	C_i (nF/cm^2)	κ (f = 100 kHz)	μ_{FE} (cm^2/Vs)		V_T (V)		ΔV_T (V)	Leakage current (A)
			−	+	−	+		
PVA	10.5	7.5	0.77	0.89	−11.52	−17.04	5.52	10^{-7}
Bilayer PR	7.1	6	0.24	0.22	−6.32	−6.33	0.01	10^{-10}

According to the published reports about various polymeric dielectrics containing hydroxyl groups, the hydroxyl group is believed as a cause of the hysteresis effect.[18,19] Concerning the α-Si TFTs with SiO_2 as insulator,[20] it is suggested that the negative oxide charge can be produced by injecting electron current into SiO_2, which causes the electron captured at the traps related to the water in the oxide. The electron capture initiates a chemical reaction, especially when neutral sodium is present. In some other reported TFTs,[21–23] the hydroxyl groups are also suggested to be electron traps. Therefore, we believe that the residual hydroxyl groups in the PVA films would capture elections, which results in the electron current injected in the PVA films and the ions such as Cr^{6+} (or Cr^{3+}) and Na^+ can easily induce this process hap-

pening. When a BCBO(III) film is inserted between organic semiconductor and PVA films, the electrons injection is restricted. As a result, the hysteresis effect and leakage current are largely reduced. On the other hand, the extra hole carriers are produced by injecting electrons from organic semiconductor into PVA films, which suggests that the OTFTs with PVA insulators have a higher mobility and a larger off-state current.

In conclusion, we have fabricated the bilayer photoresist insulator consisting of two negative photoresists. Micron-size patterns of the insulator have been directly defined only by the photolithographic process without the etching process, for example, 10-μm-wide grooves. The patterning procedure has obviously been simplified. OTFTs with the bilayer photoresist insulator have also shown a field-effect mobility of $0.78\,\mathrm{cm}^2/\mathrm{Vs}$, an on/off current ratio of about 10^6 and negligible hysteresis. Thus the bilayer insulator can be used to make flexible organic transistors with high performance and to facilitate the patterning of the insulator for the circuits and displays.

References

[1] Dimitrakopoulos C D and Malenfant P R L 2002 *Adv. Mater.* **14** 99

[2] Veres J, Ogier S, Lloyd G and de Leeuw D 2004 *Chem. Mater.* **16** 4543

[3] Yuan J F, Zhang J, Wang J, Yan X J, Yan D H and Xu W 2003 *Appl. Phys. Lett.* **82** 3967

[4] Kelley T W, Boardman L D, Dunbar T D, Muyres D V, Pellerite M J and Smith T Y P 2003 *J. Phys. Chem.* B **107** 5877

[5] Park S Y, Park M and Lee H H 2004 *Appl. Phys. Lett.* **85** 2283

[6] Muller K, Paloumpa I, Henkel K and Schmeisser D 2005 *J. Appl. Phys.* **98** 056104

[7] Onoue T, Nakamura I, Sakabe Y, Yasuda T and Tsutsui T 2006 *Jpn. J. Appl. Phys.* Ⅱ **45** L770

[8] Wang W, Shi J W, Guo S X, Zhang H M, Quan B F and Ma D G 2006 *Chin. Phys. Lett.* **23** 3108

[9] Liu P, Wu Y L, Li Y N, Ong B S and Zhu S P 2006 *J. Am. Chem. Soc.* **128** 4554

[10] Zielke D, Hubler A C, Hahn U, Brandt N, Bartzsch M, Fugmann U, Fischer T, Veres J and Ogier S 2005 *Appl. Phys. Lett.* **87** 123508

[11] Jung T, Dodabalapur A, Wenz R and Mohapatra S 2005 *Appl. Phys. Lett.* **87** 182109

[12] Hwang D K, Lee K, Kim J H, Im S, Park J H and Kim E 2006 *Appl. Phys. Lett.* **89** 093507

[13] Sze S M 2001 *Semiconductor Devices, Physics and Technology* 2nd edn (New York: Wiley)

[14] Wang Z Y, Kuang L and Gao J P 2003 *US Patent 6534250*

[15] Sheraw C D, Jia L, Gundlach D J, Klauk H and Jackson T N 2000 *42nd EMC* (Denver, Colorado, USA)

[16] Wang H, Song D, Yang J, Yu B, Geng Y and Yan D 2007 *Appl. Phys. Lett.* **90** 253510

[17] Klauk H 2006 *Organic Electronics: Materials, Manufacturing and Applications* (Weinheim: Wiley)

[18] Lee S, Koo B, Shin J, Lee E, Park H and Kim H 2006 *Appl. Phys. Lett.* **88** 162109

[19] Choi C G and Baez B S 2007 *Electrochem. Solid-State Lett.* **10** H347

[20] Nicollian E H and Brews J R 1982 *MOS Physics and Technology* (New York: Wiley)

[21] Gu G, Kane M G, Doty J E and Firester A H 2005 *Appl. Phys. Lett.* **87** 243512

[22] Kim W, Javey A, Vermesh O, Wang O, Li Y M and Dai H J 2003 *Nano Lett.* **3** 193

[23] Chua L L, Zaumseil J, Chang J F, Ou E C W, Ho P K H, Sirringhaus H and Friend R H 2005 *Nature* **434** 194